Modeling the Effect of Nut Thread Profile Angle on the Vibration-Induced Loosening of Bolted Joint Systems

Sayed A. Nassar and Xianjie Yang

Abstract The effect of the nut thread profile angle is incorporated into a nonlinear friction model for investigating vibration-induced loosening preloaded bolt–nut system that is subjected to a harmonic transverse excitation. The proposed model also takes into account the effect of frictional characteristics of engaged threads and underhead contact surfaces, thread fit class, and hole clearance, as well as on the loosening performance. Correlation is established between the relative translational movement of the bolt–nut system and the relative bending rotation of the bolt–nut system. Critical bending angle is determined by the thread fit clearance. Model results show that as compared to standard nuts with a 60° thread profile angle, M10 × 1.5 nuts with a larger thread profile angle of 120° that are engaged with standard thread M10 × 1.5 bolts (i.e., with 60° thread profile angle) showed significantly higher resistance to loosening under a harmonic transverse load. Results show also that reducing thread fit clearance (i.e., thread fit class) and/or reducing the hole clearance would increase the resistance to vibration-induced loosening.

Keywords Bolt loosening · Thread profile angle

Nomenclature

A_b	Underhead bearing area
E	Young's modulus of bolt material
F_b	Bolt tension
F_{bs}	Transverse bearing friction shear force
F_{xM}	Bolt thread shear force component along x-direction caused by bending moment
$\overline{F}_{bs}$	Bearing friction shear force ratio $\lvert F_{bs}/\mu_b q_{b0}\rvert$
F_{ts}	Thread friction shear force component along x-direction

S. A. Nassar (✉) · X. Yang
Department of Mechanical Engineering, Fastening and Joining Research Institute (FAJRI), Oakland University, Rochester, MI 48309, USA
e-mail: nassar@oakland.edu

L. F. M. da Silva et al. (eds.), *Advanced Joining Processes*,
Advanced Structured Materials 125, https://doi.org/10.1007/978-981-15-2957-3_3

$\overline{F}_{\mathrm{ts}}$	Transverse thread friction shear force ratio $\lvert F_{\mathrm{ts}}/\mu_{\mathrm{b}} q_{\mathrm{b0}}\rvert$
h_0	Engaged thread length
I	Moment of inertia for the bolt cross-sectional area
k_{b}	Bolt tensile stiffness
k_{c}	Joint compressive stiffness
L	Bolt grip length
M_{b}	Bending moment on bolt underhead surface
M_{Ns}	Bending moment on nut bearing contact surface
M_{Nt}	Bending moment on thread surface
n	Number of fully engaged threads
p	Thread pitch
q_{b}	Underhead contact pressure
q_{b0}	Average underhead contact pressure
q_{t}	Thread contact pressure
$\boldsymbol{q}_{\mathrm{t}}$	Bolt thread pressure vector
q_{t0}	Average thread contact pressure on the whole engaged threads
q'_{t0}	Average thread contact pressure at the first engaged thread
r	Radius in the polar coordinate system
r_{b}	Equivalent bolt head bearing radius
r_{maj}	Major thread radius
r_{min}	Minor thread radius
r_{o}	Maximum contact radius under the bolt head
r_{i}	Minimum contact radius under the bolt head
T_{b}	Sliding bearing friction torque under transverse cyclic excitation
$\overline{T}_{\mathrm{b}}$	Bearing friction torque ratio $\lvert T_{\mathrm{b}}/\mu_{\mathrm{b}} q_{\mathrm{b0}}\rvert$
T_{p}	Pitch torque component
T_{t}	Sliding thread friction torque under transverse cyclic excitation
$\overline{T}_{\mathrm{t}}$	Thread friction torque ratio $\lvert T_{\mathrm{t}}/\mu_{\mathrm{t}} q_{\mathrm{t0}}\rvert$
v_{bx}	Relative translation velocity along x-direction between the bolt head and the joint bearing surface
$\boldsymbol{v}_{\mathrm{A}}$	Relative translation velocity vector at Point A between the bolt thread and the nut thread
v_{Ax}	Component of $\boldsymbol{v}_{\mathrm{A}}$ along x-direction
v_{Az}	Component of $\boldsymbol{v}_{\mathrm{A}}$ along z-direction
$\boldsymbol{v}_{\mathbf{t}}$	Relative velocity vector on the contact thread surface
v_{tx}	Component of $\boldsymbol{v}_{\mathbf{t}}$ along x-direction
v_{ty}	Component of $\boldsymbol{v}_{\mathbf{t}}$ along y-direction
v_{tz}	Component of $\boldsymbol{v}_{\mathbf{t}}$ along z-direction
$\boldsymbol{w}_1$	Outward unit vector normal to the thread surface
$x, x\prime$	Cartesian x-coordinate
z, z'	Cartesian z-coordinate
α	Half of thread profile angle
β	Lead helix angle
β'	Ratio of the transverse thread friction force to the bearing friction shear force
β_{b}	Bending stiffness on bolt underhead contact area

β'_{N} Combined bending stiffness of the nut bearing surface and the engaged thread surface

β''_{N} Combined bending stiffness of the nut bearing surface and the engaged thread surface when thread relative slippage occurs

β_{Ns} Bending stiffness on nut bearing contact area

β_{Nt} Bending stiffness on bolt thread contact area

χ' Ratio $F_{\mathrm{ts}}/F_{\mathrm{bs}}$

χ'' Ratio $\Delta F_{\mathrm{ts}}/\Delta F_{\mathrm{bs}}$

δ_{b} Bolt deflection

δ_{J} External transverse displacement

δ_0 Amplitude of the transverse cyclic displacement

γ Ratio of the major radius to the minor radius of the bolt thread: $\gamma = r_{\mathrm{maj}}/r_{\mathrm{min}}$

λ_{b} Constant for bending stiffness of bolt head

λ_{Ns} Constant for bending stiffness of nut

λ_{t} Constant for thread contact pressure non-uniform distribution

η_{b} Underhead bearing translation-to-rotational sliding speed ratio ($v_{\mathrm{bx}}/\omega_{\mathrm{t}}$)

η_{N} Nut bearing translation-to-rotational sliding speed ratio ($v_{\mathrm{Nx}}/\omega_{\mathrm{t}}$)

η_{t} Thread bending-to-torsional rotational sliding speed ratio ($\omega_{\mathrm{A}}/\omega_{\mathrm{t}}$)

ρ_{M} Ratio ($\rho_{\mathrm{M}} = M_{\mathrm{Nt}}/F_{\mathrm{xM}}$), effective bending moment arm

μ_{b} Bearing friction coefficient under bolt head

μ_{t} Thread friction coefficient

θ Angular coordinate

σ'' Ratio $\Delta\delta_{\mathrm{b}}/\Delta\phi_{\mathrm{Nt}}$

ω_{A} Bending angular velocity of the bolt thread

φ_{b} Bending angle at bolt underhead

φ'_{N} Bending angle of bolt at nut threads

φ_{Ns} Nut bending angle

φ_{Nt} Relative bending angle between bolt threads and nut threads

ω_{t} Relative angular velocity of the thread surfaces about bolt axis with respect to nut thread surface

ω' Angular frequency of the transverse excitation (rad/s)

Δx Translational displacement at point A along x-direction

Δz Translational displacement at point A along z-direction

$\Delta\delta_{\mathrm{BJ}}$ Relative displacement between bolt underhead and joint

$\Delta\delta_{\mathrm{NJ}}$ Relative displacement between the nut and joint

$\Delta\varphi_{\mathrm{Nt}}$ Relative bending angle increment between the bolt threads and nut threads

$\Delta\theta_{\mathrm{A}}$ Rotation angle at point A

1 Introduction

Vibration-induced loosening of preloaded threaded fastener systems can lead to joint leakage at pressure boundaries, fatigue failure, or joint separation leading to significant warranty costs, catastrophic failure, safety risks, or loss of human life. Although there are some studies on the self-loosening of threaded fastener due to vibrations [1–13], none of the existing models has incorporated the thread profile angle as an independent variable that may have a significant effect on the vibration-induced loosening performance of preloaded threaded fastener systems. For example, Hess [7] provided a survey of some experimental and theoretical studies [4–8] on the vibration- and shock-induced loosening of threaded fasteners. The mechanism of vibration-induced loosening of threaded fasteners is primarily attributed to a reduction in the friction torque resistance, which is caused by the relative slippage between contact surfaces such as the interface between engaged threads and/or the interface between the bolt underhead and contacting joint surface [1–8]. Shoji and Sawa [13] proposed a three-dimensional finite element model to simulate the self-loosening of the threaded fastener under transverse cyclic loading. Their FEA simulation has been helpful to the understanding of the mechanics of the self-loosening process.

Nassar and Housari [14–16] developed an experimentally validated linear mathematical model for studying the loosening phenomenon in a preloaded threaded fastener system under a cyclic transverse load. The main variables in their model included the thread pitch, bolt preload, hole clearance, thread fit, bearing and thread friction coefficients, and the excitation amplitude of the cyclic transverse load. It was concluded that these parameters had a significant effect on the self-loosening of threaded fasteners. Their linear model has resulted in a linear correlation between the number of cycles-to-complete loss of bolt tension and the initial bolt preload. Subsequently, Nassar and Yang [17, 18] developed a more accurate nonlinear vibration-induced loosening model that was based on process, based on the relative slippage between two sets of contact surfaces, namely the contacting surfaces of the engaged bolt and nut threads (that had standard profile angles of 60°) and between the bearing contact between the bolt underhead and joint surfaces.

In this study, Nassar and Yang's model [17] is extended to incorporate the effect of the nut thread profile angle (as an independent design variable) on the loosening performance of a preloaded threaded joint model in which the engaged bolt threads have a standard 60° profile angle. Other variables investigated in this study include thread fit clearance, bolt hole clearance, frictional coefficients, and bolt preload level. An experimental procedure and test setup are developed for validating the proposed model.

2 Formulation of Frictional Torque and Shear Forces

This section is primarily dedicated to incorporating the engaged nut thread profile angle (as an independent variable) into the thread friction analysis of engaged bolt threads in a preloaded bolt–nut system that is subjected to a cyclic transverse load. However, frictional analysis of the bolt underhead contact surface with that of the joint surface, shown in Fig. 1, would be the same as that provided in Nassar and Yang model [17] as summarized in the following section.

2.1 Underhead Bearing Friction Analysis

Slippage and friction force illustrations on the underhead bearing contact surface are shown in Fig. 2. A transverse bearing friction shear force $\overline{F}_{\mathrm{bs}}$ and the corresponding bearing friction torque $\overline{T}_{\mathrm{b}}$ are given by Nassar and Yang [17] in terms of a newly defined speed ratio η_{b} as follows:

$$\overline{F}_{bs} = f_{3b}(\eta_b) = \left|\frac{F_{bs}}{\mu_b q_{b0}}\right| = \int_{r_i}^{r_o} r\,dr \int_0^{2\pi} \frac{(\eta_b + r\sin\theta)d\theta}{\sqrt{\eta_b^2 + r^2 + 2\eta_b r\sin\theta}} \tag{1}$$

$$\overline{T}_{\mathrm{b}} = f_{1\mathrm{b}}(\eta_{\mathrm{b}}) = \left|\frac{T_{\mathrm{b}}}{\mu_{\mathrm{b}} q_{\mathrm{b0}}}\right| = \int_{r_{\mathrm{i}}}^{r_{\mathrm{o}}} r^2 \mathrm{d}r \int_0^{2\pi} \frac{(\eta_{\mathrm{b}}\sin\theta + r)d\theta}{\sqrt{\eta_{\mathrm{b}}^2 + r^2 + 2\eta_{\mathrm{b}} r\sin\theta}} \tag{2}$$

$$\eta_{\mathrm{b}} = v_{\mathrm{bx}}/\omega_{\mathrm{t}} \tag{3}$$

where η_{b} is simply the ratio of the bolt underhead translational (sliding) speed $v_{1\mathrm{b}}$ in the x-direction to the bolt head angular (loosening) speed ω_{t}, T_{b} is the sliding

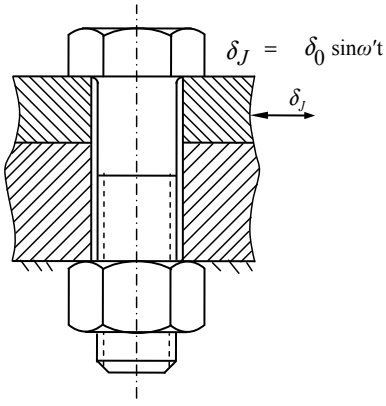

Fig. 1 Schematic of a bolt–nut model under harmonic transverse excitation

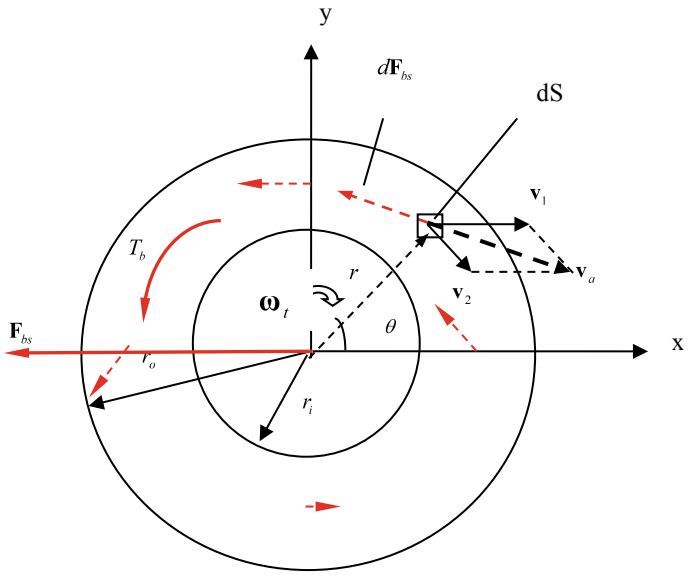

Fig. 2 Schematic diagram of underhead bearing sliding speeds bearing friction shear and torque

underhead bearing friction torque, F_{bs} is the underhead bearing friction shear force, μ_{b} is the underhead bearing friction coefficient, q_{b0} is the average underhead contact pressure, r_{i} and r_{o} are, respectively, the minimum and maximum underhead contact radii; r and θ are the polar coordinates within the underhead contact area.

Equations (1) and (2) are numerically solved for ratios $\overline{F}_{\mathrm{bs}}$ and $\overline{T}_{\mathrm{b}}$ in terms of the speed ratio η_{b} as a variable. Figure 3 shows that the bearing friction torque ratio $\overline{T}_{\mathrm{b}}$ (solid line) rapidly decreases with increasing η_{b} in the range $0 \leq \eta_{\mathrm{b}} \leq 75$, and it asymptotes to a nearzero value for $\eta_{\mathrm{b}} \geq 300$. However, the bearing shear force ratio $\overline{F}_{\mathrm{bs}}$ (dotted line) rises sharply from zero (at $\eta_{\mathrm{b}} = 0$) to a saturation value of $A_{\mathrm{b}} = \pi\left(r_{\mathrm{o}}^2 - r_{\mathrm{i}}^2\right)$ when $\eta_{\mathrm{b}} \geq 50$, approximately. The condition $\eta_{\mathrm{b}} = 0$ represents the case where the relative slippage is only due to bolt head rotation, as the force F_{bs} becomes zero in Eq. (1); the corresponding bearing friction torque in Eq. (2) is $T_{\mathrm{b}} = \mu_{\mathrm{b}} F_{\mathrm{b}} r_{\mathrm{b}}$, where F_{b} is the bolt tension and r_{b} is equivalent bearing friction radius. As $\eta_{\mathrm{b}} \to \infty$, however, the relative slippage becomes pure linear translational movement against the bearing friction force that peaks at $F_{\mathrm{bs}} = \mu_{\mathrm{b}} F_{\mathrm{b}}$ (with $T_{\mathrm{b}} = 0$).

2.2 *Incorporation of Nut Thread Profile Angle into Frictional Analysis of Engaged Thread Surfaces*

With reference to Fig. 4, since the (lead) helix angle is fairly small for standard threaded fastener products, its effect would be insignificant to the relationship

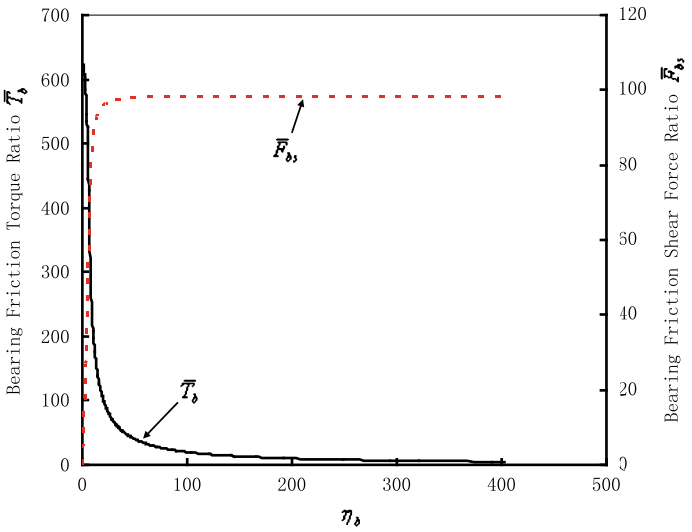

Fig. 3 Bearing friction ratios $\overline{T}_b$ and $\overline{F}_{bs}$ versus bearing speed ratio η_b for M10 × 1.5 bolt–nut model

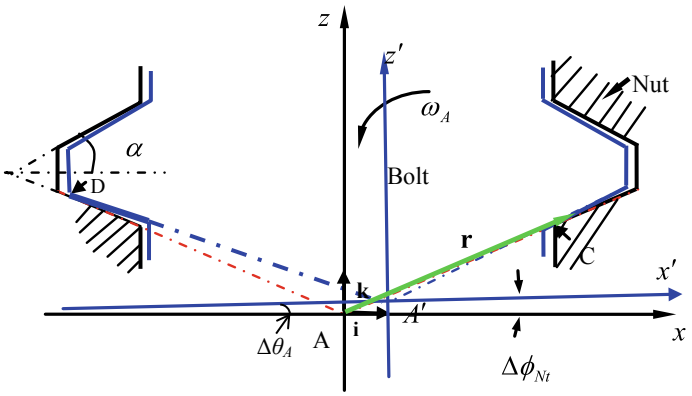

Fig. 4 Simplified 2-D schematic of local bolt and nut axes and relative slippage between engaged threads

between the x- and z-displacements at Point A and the bending angle of the thread flank. The kinetic relationship is hence established between the bending angle of the thread flank and the slippage of bolt threads with respect to the nut threads. At point A, the relative movements between the bolt and the nut are bending rotation angle $\Delta\theta_A$, and linear x- and z-displacements Δx_A and Δz_A, respectively. The key parameter $\Delta\theta_A$ for the effect of geometry clearance on the loosening performance is investigated in this study. The $x - z$ coordinate system is fixed on bolt thread while the $x' - z'$ system is fixed on nut thread. Before any relative bending rotation

occurs between bolt and nut, the original two coordinate systems coincide and have the same original point A. When a bending rotation occurs, the $x' - z'$ coordinate system has a relative translational displacement and a relative bending rotation with respect to the $x - z$ system. The relationship between the two coordinate systems is given by

$$\begin{Bmatrix} x \\ z \end{Bmatrix} = \begin{Bmatrix} \Delta x_{\mathrm{A}} \\ \Delta z_{\mathrm{A}} \end{Bmatrix} + \begin{bmatrix} \cos \Delta\theta_{\mathrm{A}} & -\sin \Delta\theta_{\mathrm{A}} \\ \sin \Delta\theta_{\mathrm{A}} & \cos \Delta\theta_{\mathrm{A}} \end{bmatrix} \begin{Bmatrix} x' \\ z' \end{Bmatrix} \tag{4}$$

For the thread surface shown in Fig. 4, we have

$$z = \pm x \tan \alpha \tag{5}$$

$$z' = \pm x' \tan \alpha \tag{6}$$

where α is half of the thread profile angle.

Equation (4) gives the following values for x and z as follows:

$$x = \Delta x_{\mathrm{A}} + x' - \Delta\theta_{\mathrm{A}} z' \tag{7}$$

$$z = \Delta z_{\mathrm{A}} + \Delta\theta_{\mathrm{A}} x' + z' \tag{8}$$

For point C on the nut thread where $x = r_{\min}$, $z = r \tan \alpha_{\min}$, $z' = x' \tan \alpha$, we have

$$\Delta x_{\mathrm{A}} + x'(1 - \Delta\theta_{\mathrm{A}} \tan \alpha) = r_{\min} \tag{9}$$

$$r_{\min} \tan \alpha = \Delta z_{\mathrm{A}} + x'(\Delta\theta_{\mathrm{A}} + \tan \alpha) \tag{10}$$

where $r_{\min}$ is the minor thread radius of the nut.

Solving Eqs. (9) and (10) and ignoring higher order terms gives the kinematic equation for point A as follows:

$$\Delta z_{\mathrm{A}} - \Delta x_{\mathrm{A}} \tan \alpha = -\Delta\theta_{\mathrm{A}} \left[r_{\min} \left(1 + \tan^2 \alpha \right) \right] \tag{11}$$

Similarly, for point D on the bolt thread (Fig. 4), using the geometric relations $x' = -r_{\mathrm{maj}}$, $z' = r_{\mathrm{maj}} \tan \alpha$, and $z = -x \tan \alpha$, where r_{maj} is the major thread radius and combing with Eq. (11) gives the x- and z-translational displacements Δx_{A} and Δz_{A} of point A and the corresponding translational velocity components v_{Ax} and v_{Az} as follows:

$$\Delta x_{\mathrm{A}} = \frac{(r_{\mathrm{maj}} + r_{\min})}{\sin 2\alpha_{\mathrm{A}}} \Delta\theta_{\mathrm{A}} \tag{12}$$

$$\Delta z_{\mathrm{A}} = \left(\frac{r_{\mathrm{maj}} - r_{\mathrm{min}}}{2} \sec^2 \alpha_{\mathrm{A}} \Delta\theta_{\mathrm{A}} \right) \tag{13}$$

$$v_{\mathrm{Ax}} = \frac{r_{\mathrm{maj}} + r_{\mathrm{min}}}{\sin 2\alpha} \Delta\theta_{\mathrm{A}} \tag{14}$$

$$v_{\mathrm{Az}} = \left(\frac{r_{\mathrm{maj}} - r_{\mathrm{min}}}{2} \right) \sec^2 \alpha \cdot \theta_{\mathrm{A}} \tag{15}$$

where ω_{A} is the time derivative $\mathrm{d}\theta_{\mathrm{A}}/\mathrm{d}t$ of the bending angle of the bolt thread.

Equations (14) and (15) characterize the relationship between the translational velocity components of point A and the bending angular speed of thread contact in x-z plane. However, the relative tangential velocity vector $\boldsymbol{v}_{\mathrm{t}}$ on the engaged threads would also include a relative rotational component about the bolt axis z. Thus, at any point on the bolt thread contact surface, the relative velocity $\boldsymbol{v}_{\mathrm{t}}$ with respect to the engaged nut threads is given by

$$\begin{aligned} \boldsymbol{v}_{\mathrm{t}} = \boldsymbol{v}_{\mathrm{A}} + (-\omega_{\mathrm{A}} \boldsymbol{j}) \times \boldsymbol{r} + (\omega_{\mathrm{t}} \boldsymbol{k}) \times \boldsymbol{r} = \left[v_{\mathrm{Ax}} - \omega_{\mathrm{A}} \left(\frac{p}{2\pi} \theta + r \tan\alpha \right) - \omega_{\mathrm{t}} r \sin\theta \right] \boldsymbol{i} \\ + \omega_{\mathrm{t}} r \cos\theta \, \boldsymbol{j} + (v_{\mathrm{Az}} + \omega_{\mathrm{A}} r \cos\theta) \boldsymbol{k} \end{aligned} \tag{16}$$

where p is the thread pitch, ω_{t} is the relative angular velocity of the thread surface about the z-axis with respect to nut thread surface.

The differential thread friction force vector $\mathrm{d}\boldsymbol{F}_{\mathrm{t}}$ on the representative area element of the engaged thread contact area is given by

$$\mathrm{d}\boldsymbol{F}_{\mathrm{t}} = \mu_{\mathrm{t}} q_{\mathrm{t}} \mathrm{d}S \frac{\boldsymbol{v}_{\mathrm{t}}}{|\boldsymbol{v}_{\mathrm{t}}|} \tag{17}$$

where μ_{t} is the thread friction coefficient, q_{t} is the thread contact pressure, and $\frac{\boldsymbol{v}_{\mathrm{t}}}{|\boldsymbol{v}_{\mathrm{t}}|}$ is a unit vector in the tangential direction. The corresponding transverse friction force component in the x-direction would be obtained from the dot product of an x-unit vector $\boldsymbol{i}$ with vector Eq. (17); the total transverse friction force F_{ts} on the thread surface would then be given by

$$\begin{aligned} F_{\mathrm{ts}} &= \iint_{\Omega_{\mathrm{thread}}} \mu_{\mathrm{t}} q_{\mathrm{t}} \frac{\boldsymbol{v}_{\mathrm{t}} \cdot \boldsymbol{i}}{|\boldsymbol{v}_{\mathrm{t}}|} \mathrm{d}S \\ &= \int_{r_{\mathrm{min}}}^{r_{\mathrm{maj}}} r \mathrm{d}r \int_{0}^{2n\pi} \frac{\mu_{\mathrm{t}} q_{\mathrm{t0}} \left\{ \frac{v_{\mathrm{Ax}}}{\omega_{\mathrm{t}}} - \frac{\omega_{\mathrm{A}}}{\omega_{\mathrm{t}}} \left(\frac{p}{2\pi} \theta + r \tan\alpha \right) - r \sin\theta \right\} \sqrt{\sec^2 \alpha + \tan^2 \beta} \mathrm{d}\theta}{\sqrt{\left[\frac{v_{\mathrm{Ax}}}{\omega_{\mathrm{t}}} - \frac{\omega_{\mathrm{A}}}{\omega_{\mathrm{t}}} \left(\frac{p}{2\pi} \theta + r \tan\alpha \right) - r \sin\theta \right]^2 + r^2 \cos^2\theta + \left[\frac{v_{\mathrm{Az}}}{\omega_{\mathrm{t}}} + \frac{\omega_{\mathrm{A}}}{\omega_{\mathrm{t}}} r \cos\theta \right]^2}} \end{aligned} \tag{18}$$

where Ω_{thread} is the overall thread contact surface area between all engaged n threads, q_{t0} is average thread contact pressure, and β is the lead helix angle of the bolt and nut threads.

Additionally, using Eq. (17), the thread friction torque increment $\mathrm{d}T_\mathrm{t}$ would be given by

$$\begin{aligned} dT_\mathrm{t} &= (\boldsymbol{r} \times \mathrm{d}\boldsymbol{F}_\mathrm{t}) \cdot \boldsymbol{k} \\ &= \begin{vmatrix} \boldsymbol{i} & \boldsymbol{j} & \boldsymbol{k} \\ r\cos\theta & r\sin\theta & r\tan\alpha + \frac{p\theta}{2\pi} \\ v_\mathrm{tx} & v_\mathrm{ty} & v_\mathrm{tz} \end{vmatrix} \cdot \boldsymbol{k} \frac{\mu_\mathrm{t} q_\mathrm{t0}}{v_\mathrm{t}} \mathrm{d}S = \left(r\cos\theta v_\mathrm{ty} - r\sin\theta v_\mathrm{tx}\right) \frac{\mu_\mathrm{t} q_\mathrm{t0}}{v_\mathrm{t}} \mathrm{d}S \end{aligned} \tag{19}$$

where v_tx, v_ty, and v_tz are the corresponding components of the sliding velocity vector $\boldsymbol{v}_t$ along x- , y- and z-directions, respectively. Taking the surface integral on the engaged thread surface Ω_thread gives the total thread friction torque T_t as follows:

$$\begin{aligned} T_\mathrm{t} &= \iint\limits_{\Omega_\mathrm{thread}} \mu_\mathrm{t} q_\mathrm{t0} \frac{\left(r\cos\theta v_\mathrm{ty} - r\sin\theta v_\mathrm{tx}\right)}{v_\mathrm{t}} \mathrm{d}S \\ &= \int_{r_\mathrm{min}}^{r_\mathrm{maj}} r\mathrm{d}r \int_0^{2n\pi} \frac{\mu_\mathrm{t} q_\mathrm{t0} \left\{ r^2 - r\sin\theta \left[\frac{v_\mathrm{Ax}}{\omega_\mathrm{t}} - \frac{\omega_\mathrm{A}}{\omega_\mathrm{t}} \left(\frac{p}{2\pi}\theta + r\tan\alpha \right) \right] \right\} \sqrt{\sec^2\alpha + \tan^2\beta}\,\mathrm{d}\theta}{\sqrt{\left[\frac{v_\mathrm{Ax}}{\omega_\mathrm{t}} - \frac{\omega_\mathrm{A}}{\omega_\mathrm{t}} \left(\frac{p}{2\pi}\theta + r\tan\alpha \right) - r\sin\theta \right]^2 + r^2\cos^2\theta + \left[\frac{v_\mathrm{Az}}{\omega_\mathrm{t}} + \frac{\omega_\mathrm{A}}{\omega_\mathrm{t}} r\cos\theta \right]^2}} \end{aligned} \tag{20}$$

Using Eqs. (18) and (20) and following a procedure similar to that employed in Sect. 2.1, the transverse thread force $\overline{F}_\mathrm{ts}$ and thread torque $\overline{T}_\mathrm{t}$ are obtained as follows:

$$\overline{F}_\mathrm{ts} = \frac{F_\mathrm{ts}}{n\mu_\mathrm{t} q_\mathrm{t0}} = \int_{r_\mathrm{min}}^{r_\mathrm{maj}} r\mathrm{d}r \int_0^{2\pi} \frac{\left\{ \left[\frac{r_\mathrm{maj} + r_\mathrm{min}}{\sin 2\alpha} - \left(\frac{p}{2\pi}\theta + r\tan\alpha \right) \right] \eta_\mathrm{t} - r\sin\theta \right\} \sqrt{\sec^2\alpha + \tan^2\beta}\,\mathrm{d}\theta}{\sqrt{\left\{ \left[\frac{r_\mathrm{maj} + r_\mathrm{min}}{\sin 2\alpha} - \left(\frac{p}{2\pi}\theta + r\tan\alpha \right) \right]^2 + \left[\frac{r_\mathrm{maj} - r_\mathrm{min}}{2} \sec^2\alpha + r\cos\theta \right]^2 \right\} \eta_\mathrm{t}^2 + r^2 - 2 \left[\frac{r_\mathrm{maj} + r_\mathrm{min}}{\sin 2\alpha} - \left(\frac{p}{2\pi}\theta + r\tan\alpha \right) \right] \eta_\mathrm{t} r\sin\theta}} \tag{21}$$

$$\overline{T}_\mathrm{t} = \frac{T_\mathrm{t}}{n\mu_\mathrm{t} q_\mathrm{t0}} = \int_{r_\mathrm{min}}^{r_\mathrm{maj}} r\mathrm{d}r \int_0^{2\pi} \frac{\left\{ r^2 + \eta_\mathrm{t} \left(\frac{p\theta}{2\pi} + r\tan\alpha - \frac{r_\mathrm{maj} + r_\mathrm{min}}{\sin 2\alpha} \right) r\sin\theta \right\} \sqrt{\sec^2\alpha + \tan^2\beta}\,\mathrm{d}\theta}{\sqrt{\left\{ \left[\frac{r_\mathrm{maj} + r_\mathrm{min}}{\sin 2\alpha} - \left(\frac{p}{2\pi}\theta + r\tan\alpha \right) \right]^2 + \left[\frac{r_\mathrm{maj} - r_\mathrm{min}}{2} \sec^2\alpha + r\cos\theta \right]^2 \right\} \eta_\mathrm{t}^2 + r^2 - 2 \left[\frac{r_\mathrm{maj} + r_\mathrm{min}}{\sin 2\alpha} - \left(\frac{p}{2\pi}\theta + r\tan\alpha \right) \right] \eta_\mathrm{t} r\sin\theta}} \tag{22}$$

where the bending-to-torsional angular (sliding) speed ratio η_t on the threads is defined by

$$\eta_\mathrm{t} = \frac{\omega_\mathrm{A}}{\omega_\mathrm{t}} \tag{23}$$

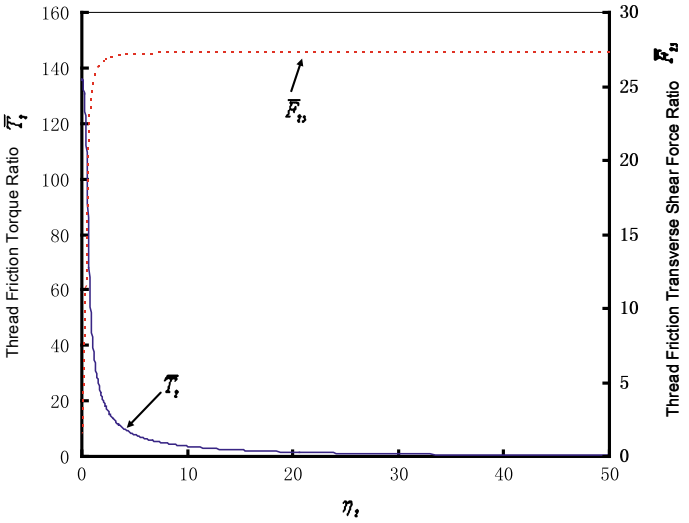

Fig. 5 Thread friction ratios $\overline{T}_t$ and $\overline{F}_{ts}$ versus thread speed ratio η_t for M10 × 1.5 bolt–nut model

Integral Eqs. (21) and (22) are numerically solved for $\overline{F}_{ts}(f_{3t}(\eta_t))$ and $\overline{T}_t(f_{1t}(\eta_t))$ in terms of the bending-to-torsional rotational sliding speed ratio η_t. Figure 5 shows that the (sliding) thread friction torque $\overline{T}_t$ (solid line) decreases rapidly in the range $0 \leq \eta_t \leq 20$; its value approaches zero for $\eta_t > 30$, although the limit of the right-hand side of Eq. (22) goes to zero as $\eta_t \to \infty$. The thread friction transverse shear force ratio $\overline{F}_{ts}$ (dotted line) rises rapidly from zero at $\eta_t = 0$ to its saturation value.

Under the transverse cyclic load (Fig. 1), intermittent vibration-induced loosening of the bolt would only occur when the value of system's pitch torque component $T_p = \frac{p}{2\pi} F_b$ from bolt–nut preloading [19] exceeds the sum of the sliding bearing friction torque component T_b and the sliding thread friction torque component T_t. From Eqs. (2) and (22), the condition for vibration-induced bolt loosening is given by

$$\left[T_p = \frac{p}{2\pi} F_b\right] > \left[\left(T_b = \mu_b n q_{b0} \overline{T}_b\right) + \left(T_t = \mu_t n q_{t0} \overline{T}_t\right)\right] \tag{24}$$

2.3 *Transverse Shear Force on Bolt Thread Surface Due to Bending*

The contact pressure distribution on preloaded engaged thread surfaces varies significantly along the bolt axis, with the highest contact pressure being on the first fully engaged thread near the face of the nut [20, 21]. Thread contact pressure rapidly

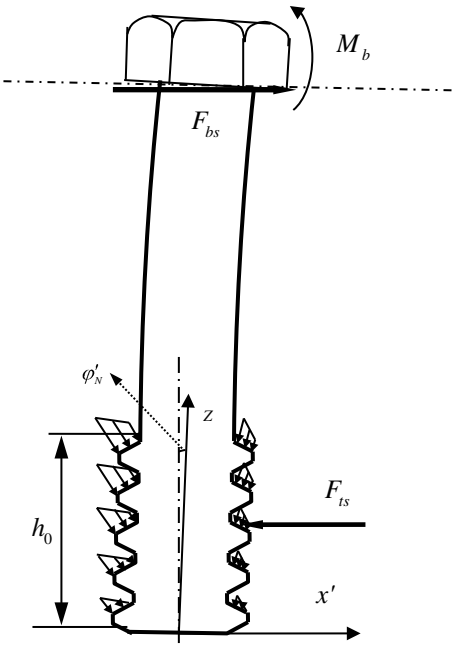

Fig. 6 Schematic of thread contact pressure distribution on threads

decreases with the distance from the first fully engaged thread. Bolt bending due to the externally applied transverse excitation would cause non-uniform distribution on each thread surface as illustrated by Fig. 6. A nonlinearly varying thread contact pressure vector $\boldsymbol{q}_{\mathrm{t}}$ is assumed as follows:

$$\boldsymbol{q}_{\mathrm{t}} = -\left[1 - \frac{p\theta}{3\pi h_0} - \frac{1}{3}\left(\frac{p\theta}{2\pi h_0}\right)^2\right]\left(q'_{\mathrm{t}0} + \lambda_{\mathrm{t}}\varphi_{\mathrm{Nt}}\frac{r\cos\theta}{r_{\mathrm{maj}}}\right)\boldsymbol{w}_1 \tag{25}$$

where $q'_{\mathrm{t}0}$ is the average thread contact pressure on the first engaged thread surface, z is the axial location, x is the transverse location, λ_{t} is a constant, φ_{Nt} is the bending angle at bolt threads, h_0 is the thread engagement length, $\boldsymbol{w}_1$ is the unit vector normal to the thread surface, which is given by

$$\boldsymbol{w}_1 = \frac{-(\tan\alpha\cos\theta + \tan\beta\sin\theta)\boldsymbol{i} - (\tan\alpha\sin\theta - \tan\beta\cos\theta)\boldsymbol{j} + \boldsymbol{k}}{\sqrt{\sec^2\alpha + \tan^2\beta}} \tag{26}$$

The bolt preload F_{b} is obtained by integrating the contact pressure overall engaged thread surfaces as follows:

$$F_b = \iint\limits_{\Omega_{\mathrm{thread}}} |\mathrm{q}_t \cdot \mathrm{k}|ds \approx \int\limits_{r_{\mathrm{maj}}}^{r_{\mathrm{min}}} rdr \int\limits_0^{2n\pi} q'_{t0}\left[1 - \frac{p\theta}{3\pi h_0} - \frac{1}{3}\left(\frac{p\theta}{2\pi h_0}\right)^2\right]d\theta$$

$$\approx q_t' 0 n\pi \left(r_{\text{maj}}^2 - r_{\text{min}}^2\right)\left\{1 - \frac{1}{3} - \frac{1}{9}\right\} = \frac{5}{9} q_t' 0 n\pi \left(r_{\text{maj}}^2 - r_{\text{min}}^2\right) \tag{27}$$

Thus, the average thread contact pressure q_{t0}' on the surface of the first engaged thread would be given by

$$q_{\text{t0}}' = \frac{9F_{\text{b}}}{5n\pi\left(r_{\text{maj}}^2 - r_{\text{min}}^2\right)} \tag{28}$$

The total transverse thread shear force component F_{xM} (along x-direction) caused by the non-uniform pressure distribution on all thread surfaces would be through dot product by the unit vector $\mathbf{i}$ as follows:

$$\begin{aligned} F_{\text{xM}} &= \iint\limits_{\Omega_{\text{thread}}} \left|\boldsymbol{q}_{\text{t}} \cdot \boldsymbol{i}\right| \text{d}s \\ &\approx \int\limits_{r_{\text{min}}}^{r_{\text{maj}}} r\,\text{d}r \int\limits_{0}^{2n\pi} (\tan\alpha\cos\theta \\ &+ \tan\beta\sin\theta)\left[1 - \frac{p\theta}{3\pi h_0} - \frac{1}{3}\left(\frac{p\theta}{2\pi h_0}\right)^2\right]\lambda_{\text{t}}\varphi_{\text{Nt}}\left(\frac{r\cos\theta}{r_{\text{maj}}}\right)d\theta \\ &\approx \frac{5n\pi\tan\alpha\lambda_{\text{t}}\varphi_{\text{nt}}}{27 r_{\text{maj}}}\left(r_{\text{maj}}^3 - r_{\text{min}}^3\right) \end{aligned} \tag{29}$$

The corresponding bending moment M_{Nt} caused by the non-uniform thread contact pressure $\boldsymbol{q}_{\text{t}}$ about y-axis at the nut axis center is formulated as follows:

$$\begin{aligned} M_{\text{Nt}} &= \iint\limits_{\Omega_{\text{xy}}} \left\{r\cos\theta + \left[r\tan\alpha + \tfrac{\theta}{2\pi}p\right](\tan\alpha\cos\theta + \tan\beta\sin\theta)\right\}\left[1 - \tfrac{p\theta}{3\pi h_0}\right. \\ &\quad \left. - \tfrac{1}{3}\left(\tfrac{p\theta}{2\pi h_0}\right)^2\right]\lambda_{\text{t}}\varphi_{\text{Nt}}\tfrac{r\cos\theta}{r_{\text{maj}}} r\,\text{d}r\,\text{d}\theta = \tfrac{\lambda_{\text{t}}\varphi_{\text{nt}}}{r_{\text{mx}}} \\ &\int_{r_{\text{min}}}^{r_{\text{maj}}} r^3\,\text{d}r \int\limits_{0}^{2n\pi} [\cos\theta - (\theta\tan\beta + \tan\alpha)(\tan\alpha\cos\theta + \tan\beta\sin\theta)]\cos\theta\, d\theta \\ &\approx \tfrac{n\pi\lambda_{\text{t}}\varphi_{\text{Nt}}}{r_{\text{maj}}}\left(r_{\text{maj}}^4 - r_{\text{min}}^4\right)\left[\tfrac{5}{36}\sec^2\alpha + \tfrac{7n\pi}{72}\tan\alpha\tan\beta\right] = \beta_{\text{Nt}}\varphi_{\text{N}t} \end{aligned} \tag{30}$$

where Ω_{xy} is the projected area of the thread contact area on x-y plane, and the bending stiffness β_{Nt} of the engaged threads is given by

$$\beta_{\text{Nt}} \approx \frac{n\pi\lambda_{\text{t}}}{r_{\text{maj}}}\left(r_{\text{maj}}^4 - r_{\text{min}}^4\right)\left[\frac{5}{36}\sec^2\alpha + \frac{7n\pi}{72}\tan\alpha\tan\beta\right] \tag{31}$$

From Eqs. (29) and (30), the relationship between the thread shear force F_{xM} and the corresponding bending moment M_{Nt} on the thread surfaces may be expressed as follows:

$$F_{\mathrm{xM}} = \frac{M_{\mathrm{Nt}}}{\rho_{\mathrm{M}}}\,,\ \rho_{\mathrm{M}} = \frac{r_{min}\left(\gamma^4 - 1\right)\left(30\sec^2\alpha + 21n\pi\tan\alpha\tan\beta\right)}{40\tan\alpha\left(\gamma^3 - 1\right)} \tag{32}$$

where the effective bending moment arm ρ_{M} and the number of fully engaged threads in Fig. 6 is $n = h_0/p$.

As long as bolt bending (due to M_{Nt}) does not consume the hole clearance (to causes direct contact between the bolt shank and the internal surface of the hole), the thread friction shear force component F_{ts} in the x-direction would be given by

$$F_{\mathrm{ts}} = F_{\mathrm{bs}} + M_{\mathrm{Nt}}/\rho_{\mathrm{M}} \tag{33}$$

2.4 Rate of Bolt Loosening Due to Cyclic Transverse Load

In this section, various scenarios are used to formulate the rate of vibration-induced loosening per cycle in a preloaded bolt–nut model that incorporates the nut thread profile angle as an independent variable. Classical elastic beam theory is used in connection with the preceding formulation of the bearing shear force F_{bs}, bolt bending moment M_{b}, and twisting torque components T_{b} and T_{tp}.

Scenario I: No slippage on any contact surfaces (bolt underhead, nut face, or thread surfaces)
The bolt deflection δ_{b} and the bending angle φ_{b} at the junction with the bolt head (Fig. 6) are, respectively, given by

$$\delta_{\mathrm{b}} = \frac{F_{\mathrm{bs}}L^3}{3EI} - \frac{M_{\mathrm{b}}L^2}{2EI} + \varphi'_{\mathrm{N}}L \tag{34}$$

$$\varphi_{\mathrm{b}} = \frac{F_{\mathrm{bs}}L^2}{2EI} - \frac{M_{\mathrm{b}}L}{EI} + \varphi'_{\mathrm{N}} \tag{35}$$

where L is bolt grip length, E is Young's modulus of bolt material, I is moment of inertia of the bolt cross-sectional area, M_{b} is bending moment acting at the bolt underhead surface, the angle φ'_{N} is the sum of the nut rotational angle φ_{Ns} and the relative bending angle φ_{Nt} between the bolt threads and nut threads as follows:

$$\varphi'_{\mathrm{N}} = \varphi_{\mathrm{Ns}} + \varphi_{\mathrm{Nt}} \tag{36}$$

As the bolt and nut have small masses, when the transverse vibration frequency and excitation amplitude are not very high, the dynamic inertia force and moment can be ignored. The equilibrium conditions of the bolt–nut connection can make the following relationships

$$F_{\mathrm{bs}}L = M_{\mathrm{b}} + M_{\mathrm{Ns}}, \quad F_{\mathrm{bs}} = F_{\mathrm{Ns}}, \quad M_{\mathrm{Ns}} = M_{\mathrm{Nt}} \tag{37}$$

where F_{Ns} is the shear force on the nut bearing contact surface along x-direction, and M_{Ns} is the bending moment on nut bearing contact surface.

The relationships between the bending moments and the corresponding rotations of the bolt underhead, nut bearing surface and the engaged threads are assumed to be expressed as follows:

$$M_{\mathrm{b}} = \beta_{\mathrm{b}}\varphi_{\mathrm{b}}, \quad M_{\mathrm{Ns}} = \beta_{\mathrm{Ns}}\varphi_{\mathrm{Ns}}, \quad M_{\mathrm{Nt}} = \beta_{\mathrm{Nt}}\varphi_{\mathrm{Nt}} \tag{38}$$

where β_{b}, β_{Ns}, and β_{Nt} are, respectively, the bending stiffness of bolt underhead to joint, nut bearing-to-joint, and bolt threads-to-nut. The combined bending stiffness $\beta_{\mathrm{N}}^{'}$ of the nut bearing-to-joint and the engaged threads to nut is expressed as follows:

$$\frac{1}{\beta_{\mathrm{N}}^{'}} = \frac{1}{\beta_{\mathrm{Ns}}} + \frac{1}{\beta_{\mathrm{Nt}}} \tag{39}$$

From Eqs. (35) to (38), the following equations are also obtained

$$\delta_{\mathrm{b}} = \frac{F_{\mathrm{bs}}L^3}{3EI}\left\{1 + \frac{\frac{3EI}{L\beta_{\mathrm{N}}^{'}} - \frac{3L}{4EI}\beta_{\mathrm{b}}}{1 + \frac{\beta_{\mathrm{b}}L}{EI} + \frac{\beta_{\mathrm{b}}}{\beta_{\mathrm{N}}^{'}}}\right\}, \quad \varphi_{\mathrm{b}} = \frac{3EI\delta_{\mathrm{b}}}{L^2}\frac{\frac{L}{2EI} + \frac{1}{\beta_{\mathrm{N}}^{'}}}{1 + \frac{3EI}{\beta_{\mathrm{N}}^{'}L} + \frac{\beta_{\mathrm{b}}L}{4EI} + \frac{\beta_{\mathrm{b}}}{\beta_{\mathrm{N}}^{'}}},$$
$$\varphi_{\mathrm{Nt}} = \frac{3EI\delta_{\mathrm{b}}}{\beta_{\mathrm{Nt}}L^2}\frac{1 + \frac{\beta_{\mathrm{b}}L}{2EI}}{1 + \frac{3EI}{\beta_{\mathrm{N}}^{'}L} + \frac{\beta_{\mathrm{b}}L}{4EI} + \frac{\beta_{\mathrm{b}}}{\beta_{\mathrm{N}}^{'}}} \tag{40}$$

If the bolt underhead and nut bearing contact pressures are assumed to vary linearly along the x-direction (Fig. 6), the bending moments M_{b} and M_{Ns} are given by

$$M_{\mathrm{b}} = \frac{\lambda_{\mathrm{b}}\pi}{4r_{\mathrm{e}}}\left(r_{\mathrm{e}}^4 - r_{\mathrm{i}}^4\right)\varphi_{\mathrm{b}} = \beta_{\mathrm{b}}\varphi_{\mathrm{b}}, \quad M_{\mathrm{Ns}} = \frac{\lambda_{\mathrm{Ns}}\pi}{4r_{\mathrm{Ne}}}\left(r_{\mathrm{Ne}}^4 - r_{\mathrm{Ni}}^4\right)\varphi_{\mathrm{Ns}} = \beta_{\mathrm{Ns}}\varphi_{\mathrm{Ns}} \tag{41}$$

where λ_{b} and λ_{Ns} are constants which affect β_{b} and β_{Ns}, respectively, and they are presented as follows:

$$\beta_{\mathrm{b}} = \frac{\lambda_{\mathrm{b}}\pi}{4r_{\mathrm{e}}}\left(r_{\mathrm{e}}^4 - r_{\mathrm{i}}^4\right), \quad \beta_{\mathrm{Ns}} = \frac{\lambda_{\mathrm{Ns}}\pi}{4r_{\mathrm{Ne}}}\left(r_{\mathrm{Ne}}^4 - r_{\mathrm{Ni}}^4\right) \tag{42}$$

Equation (40) shows the linear relationship between the bolt deflection δ_{b} and the underhead friction shear force F_{bs} given by Eq. (1), which would also determine the value of the sliding underhead friction torque T_{b}. Similarly, Eqs. (34), (38), and (40) give the transverse shear force F_{ts} on the engaged threads in terms of F_{bs} as follows:

$$F_{\mathrm{ts}} = F_{\mathrm{bs}} + M_{\mathrm{Nt}}/\rho_{\mathrm{M}} = F_{\mathrm{bs}}\left[1 + \left(\frac{L}{\rho_{\mathrm{M}}}\right)\frac{1 + \frac{\beta_{\mathrm{b}}L}{2EI}}{1 + \frac{\beta_{\mathrm{b}}L}{EI} + \frac{\beta_{\mathrm{b}}}{\beta_{\mathrm{N}}^{'}}}\right] = \chi' F_{\mathrm{bs}},$$

$$\chi' = \left[1 + \left(\frac{L}{\rho_{\mathrm{M}}}\right)\frac{1 + \frac{\beta_{\mathrm{b}}L}{2EI}}{1 + \frac{\beta_{\mathrm{b}}L}{EI} + \frac{\beta_{\mathrm{b}}}{\beta'_{\mathrm{N}}}}\right] \tag{43}$$

The expression for χ' in Eq. (43) represents the ratio of the thread friction force F_{ts} to the bearing friction shear force F_{bs}, which is obviously larger than 1.

Scenario II: Slippage only on the engaged thread surfaces (without slippage under the bolt head or the nut face)

When slippage occurs on the thread contact surface (as the contact friction force has reached its critical value), the increment $\Delta\delta_{\mathrm{b}}$ in bolt deflection and the corresponding bending angle increment $\Delta\varphi_{\mathrm{b}}$ of the bolt axis at the bolt head is, respectively, given by

$$\Delta\delta_{\mathrm{b}} = \frac{\Delta F_{\mathrm{bs}}L^3}{3EI} - \frac{\Delta M_{\mathrm{b}}L^2}{2EI} + \Delta\varphi'_{\mathrm{N}}L, \quad \Delta\varphi_{\mathrm{b}} = \frac{\Delta F_{\mathrm{bs}}L^2}{2EI} - \frac{\Delta M_{\mathrm{b}}L}{EI} + \Delta\varphi'_{\mathrm{N}} \tag{44}$$

Following the same procedure in scenario I, expressions for $\Delta\delta_{\mathrm{b}}$, $\Delta\varphi_{\mathrm{b}}$, φ_{Nt}, and F_{ts} are obtained as follows:

$$\begin{aligned}
\Delta\delta_{\mathrm{b}} &= \tfrac{\Delta F_{\mathrm{bs}}L^3}{3EI}\left\{1 + \frac{\frac{3EI}{L\beta''_{\mathrm{N}}} - \frac{3L}{4EI}\beta_{\mathrm{b}}}{1 + \frac{\beta_{\mathrm{b}}L}{EI} + \frac{\beta_{\mathrm{b}}}{\beta'_{\mathrm{N}}}}\right\},\\
\Delta\varphi_{\mathrm{b}} &= \left(\tfrac{3EI\Delta\delta_{\mathrm{b}}}{L^2}\right)\frac{\frac{L}{2EI} + \frac{1}{\beta''_{\mathrm{N}}}}{1 + \frac{3EI}{\beta''_{\mathrm{N}}L} + \frac{\beta_{\mathrm{b}}L}{4EI} + \frac{\beta_{\mathrm{b}}}{\beta''_{\mathrm{N}}}},\\
\Delta\varphi_{\mathrm{Nt}} &= \left(\tfrac{3EI\Delta\delta_{\mathrm{b}}}{\beta'_{\mathrm{Nt}}L^2}\right)\frac{1 + \frac{\beta_{\mathrm{b}}L}{2EI}}{1 + \frac{3EI}{\beta''_{\mathrm{N}}L} + \frac{\beta_{\mathrm{b}}L}{4EI} + \frac{\beta_{\mathrm{b}}}{\beta''_{\mathrm{N}}}} = \Delta\delta_{\mathrm{b}}/\sigma'',\\
\Delta F_{\mathrm{ts}} &= \Delta F_{\mathrm{bs}} + \tfrac{\Delta M_{\mathrm{Nt}}}{\rho_{\mathrm{M}}} = \Delta F_{\mathrm{bs}}\left[1 + \left(\tfrac{L}{\rho_{\mathrm{M}}}\right)\frac{1 + \frac{\beta_{\mathrm{b}}L}{2EI}}{1 + \frac{\beta_{\mathrm{b}}L}{EI} + \frac{\beta_{\mathrm{b}}}{\beta''_{\mathrm{N}}}}\right]\\
&= \chi''\Delta F_{\mathrm{bs}}
\end{aligned} \tag{45}$$

where β'_{Nt} (which much less than β_{Nt} in Eq. (39)) is the contact bending stiffness of the bolt threads with respect to the nut threads as relative slippage between engaged threads occurs, and β''_{N} is the combined bending stiffness (bolt threads to nut and nut to clamped joint) during the slippage of the threads given by

$$\frac{1}{\beta''_{\mathrm{N}}} = \frac{1}{\beta_{\mathrm{Ns}}} + \frac{1}{\beta'_{\mathrm{Nt}}}, \tag{46}$$

and σ'' is given by

$$\sigma'' = \frac{1 + \frac{3EI}{\beta''_{\mathrm{N}}L} + \frac{\beta_{\mathrm{b}}L}{4EI} + \frac{\beta_{\mathrm{b}}}{\beta''_{\mathrm{N}}}}{1 + \frac{\beta_{\mathrm{b}}L}{2EI}}\left(\frac{\beta'_{\mathrm{Nt}}L^2}{3EI}\right) \tag{47}$$

A linear relationship exists in Eq. (45) between the incremental bolt deflection $\Delta\delta_b$ and the incremental underhead shear force ΔF_{bs} . The total value of the bearing transverse friction shear force F'_{bs} would be

$$F'_{bs} = F_{bs} + \Delta F_{bs} \tag{48}$$

Similar to Scenario 1, the value of the underhead friction shear force F'_{bs} will determine the value of the sliding underhead friction torque T_b by using Eqs. (1) and (2). Equation (45) also gives the relative bending angle increment $\Delta\varphi_{Nt}$ between the bolt threads and nut threads in terms of bolt deflection increment $\Delta\delta_b$. If the thread angle increment $\Delta\varphi_{Nt}$ reaches its critical value $\Delta\varphi_{Ntcr}$, which is determined by the thread geometry and the class of thread fit, slippage between the engaged threads would stop (i.e., loosening rotation would stop under this condition). Further increase of the transverse displacement of the joint would only cause relative transverse slippage between the nut face and the joint surface, which does not cause any loosening.

Scenario III: Relative slippage occurs simultaneously between all of the three sets of contact surfaces (bolt underhead–joint, nut face–joint, and engaged bolt–nut threads)

As outlined in Scenarios I and II, bolt loosening will only take place when each of the two surfaces is sliding against its respective contact. That requires the bolt underhead surface to be sliding against the contacting joint surface, which must also be simultaneous with relative sliding occurring between the contact surfaces of engaged threads. This is further explained in the following two sections:

(1) **Simultaneous slippage on the bolt underhead–joint and the engaged bolt–nut thread surfaces (without nut face slippage)**

The relative displacement $\Delta\delta_{BJ}$ between bolt underhead and the fixed joint is given by

$$\Delta\delta_{BJ} = \delta_J - \Delta\delta_b - \Delta x_A = \delta_J - \sigma''\Delta\varphi_{Nt} - \Delta x_A \tag{49}$$

$$\delta_J = \delta_0 \sin\omega' t \tag{50}$$

where δ_b is the bolt deflection that corresponds to the relative displacement between the bolt underhead and its threaded end, δ_J is the cyclic joint transverse excitation, Δx_A is the relative displacement of the bolt threads, $\Delta\varphi_{Nt}$ is the relative bolt thread bending angular increment with respect to nut, δ_0 is the amplitude of cyclic transverse excitation, and ω' is the angular frequency of the transverse excitation.

Differentiating Eq. (49) with respect to time, and the translational-to-angular speed ratios η_b and η_t as defined earlier (Sects. 2.1 and 2.2) gives bolt rotational speed ω_t of bolt threads relative to engaged nut threads as follows:

$$\omega_{\mathrm{t}} = \frac{\dot{\delta}_{\mathrm{J}}}{\eta_{\mathrm{b}} + \eta_{\mathrm{t}}\left(\frac{r_{\mathrm{maj}}+r_{\mathrm{min}}}{\sin 2\alpha} + \sigma''\right)} \tag{51}$$

The relative bending rotation increment $\Delta\varphi_{\mathrm{Nt}}$ with respect to the nut is obtained by integration as follows:

$$\Delta\varphi_{\mathrm{Nt}} = \int_{t_1}^{t} \omega_{\mathrm{A}}\mathrm{d}t = \int_{t_1}^{t} \eta_{\mathrm{t}}\omega_{\mathrm{t}}\mathrm{d}t \tag{52}$$

where t_1 indicated the start of loosening and t is current time (i.e., loosening duration $= t - t_1$).

The critical value $\Delta\varphi_{\mathrm{Ntcr}}$, which is the maximum bending angle between the bolt and the nut, is approximately determined by

$$\Delta\varphi_{\mathrm{Ntcr}} = \frac{\Delta d_{\mathrm{th}}}{\sqrt{d^2 + H^2}} \tag{53}$$

where Δd_{th} is the thread fit clearance between the bolt threads and nut threads (Fig. 7: based on pitch diameter), d is the bolt nominal diameter, H is the thread engagement length (Fig. 6). If $\Delta\varphi_{\mathrm{Nt}}$ reaches its critical value $\Delta\varphi_{\mathrm{Ntcr}}$, the bolt threads cannot have further relative bending angle increment with nut threads. The critical value $\Delta\varphi_{\mathrm{Ntcr}}$ is dependent on the thread clearance Δd_{th} (fit class), the thread engagement length H, and the thread major–minor diameters. As a result, $\Delta\varphi_{\mathrm{Ntcr}}$ would be proportional to the thread fit clearance, and it would decrease with the increasing the thread engagement length H and thread diameter. The horizontal resisting force would balance the external transverse shear force. The thread friction torque will increase significantly by the transverse resistant force. Under this scenario, the loosening condition is not satisfied and the loosening rotation of the bolt will stop.

On the other hand, if the absolute value $|\Delta\delta_{\mathrm{BJ}}|$ of the relative displacement reaches its critical value, which is equal to the joint hole diameter clearance Δd_{h}, the bolt shank will contact with the cylindrical surface of the hole. The contact pressure on the hole surface will produce additional friction torque resistance to the bolt loosening rotation. The additional friction torque can prevent the self-loosening of the threaded fastener.

If $\Delta\varphi_{\mathrm{Nt}} < \Delta\varphi_{\mathrm{Ntcr}}$ and $|\Delta\delta_{\mathrm{BJ}}| < \Delta d_{\mathrm{h}}$, the incremental clamp load loss $\mathrm{d}F_{\mathrm{b}}$ due to loosening caused by the transverse cyclic loading is given by

$$\mathrm{d}F_{\mathrm{b}} = \frac{k_{\mathrm{b}}k_{\mathrm{c}}}{k_{\mathrm{b}}+k_{\mathrm{c}}}\frac{p}{2\pi}\omega_{\mathrm{t}}\mathrm{d}t = \frac{k_{\mathrm{b}}k_{\mathrm{c}}}{k_{\mathrm{b}}+k_{\mathrm{c}}}\frac{p}{2\pi}\frac{\left|\dot{\delta}_{\mathrm{J}}\right|\mathrm{d}t}{\eta_{\mathrm{b}} + \eta_{\mathrm{t}}\left(\sigma'' + \frac{r_{\mathrm{maj}}+r_{\mathrm{min}}}{\sin 2\alpha}\right)} \tag{54}$$

(2) **Simultaneous slippage on the joint–nut face and bolt–nut engaged thread surfaces (without slippage on the bolt underhead surface)**

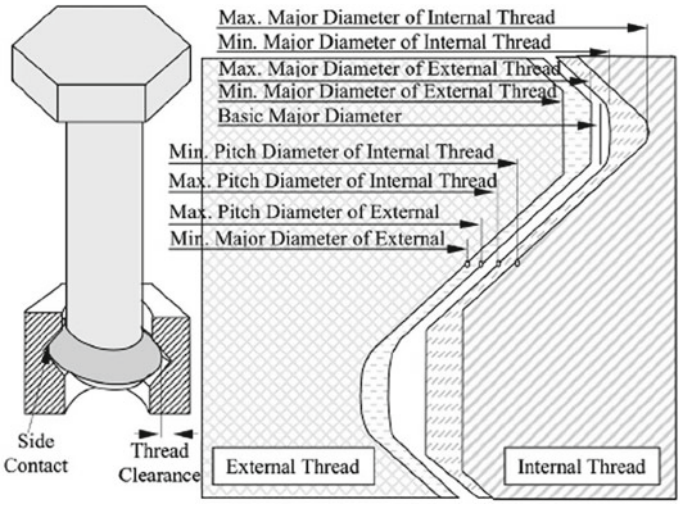

Fig. 7 Schematic of the thread clearance between engaged bolt and nut threads

The relative displacement $\Delta\delta_{NJ}$ for the nut and the joint is given by Eq. (49). If $\Delta\varphi_{Nt} < \Delta\varphi_{Ntcr}$ and $|\Delta\delta_{NJ}| < \Delta d_h$, the incremental clamp load loss dF_b due to the loosening caused by the transverse cyclic loading would be given by

$$\begin{aligned} \mathrm{d}F_b &= \frac{k_b k_c}{k_b + k_c}\left(\frac{p}{2\pi}\right)\omega_t \mathrm{d}t \\ &= \frac{k_b k_c}{k_b + k_c}\left(\frac{p}{2\pi}\right)\frac{\left|\dot{\delta}_J\right|\mathrm{d}t}{\eta_N + \eta_t\left(\sigma'' + \frac{r_{maj}+r_{min}}{\sin 2\alpha}\right)}, \quad \text{with} \quad \eta_N = v_{Nx}/\omega_t \end{aligned} \tag{55}$$

3 Results and Discussion

Figures 8, 9, 10, 11, 12, 13, and 14 show the proposed model prediction of loosening performance represented by Eq. (54), and the corresponding experimental validation, of a steel M10 × 1.5 Class 8 bolt–nut system (Fig. 1) that is subjected to harmonic transverse displacement with amplitude $\delta_0 = 0.71$ mm. Typical values of 200 MPa and 0.3 are, respectively, used for Young's modulus and Poisson's ratio. While the bolt thread profile angle is fixed in this study (at its standard 60° value), two different values are investigated for the engaged nut thread profile angle, namely the non-standard profile with $2\alpha = 120°$ and the standard nut thread are profile angle with $2\alpha = 60°$. Commercially available nuts with nonstandard profile angle $2\alpha = 120°$ are referred to as Spiralock nuts [7]. Coefficients of underhead bearing friction μ_b, thread friction μ_t were determined from separate precision torque-tension tests; their

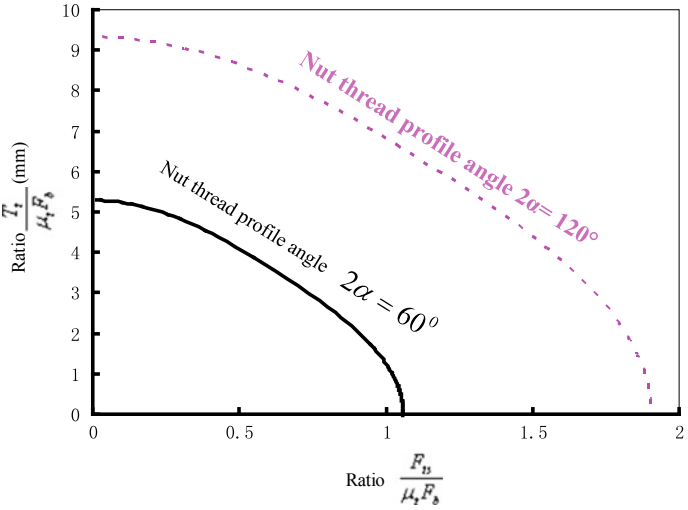

Fig. 8 Thread friction torque ratio $\overline{T}_t = \frac{T_t}{\mu_t F_b}$ versus thread friction transverse shear ratio $\overline{F}_{ts} = \frac{F_{ts}}{\mu_t F_b}$ (for nonstandard nut profile angle $2\alpha = 120°$ and standard nut profile angle $2\alpha = 60°$)

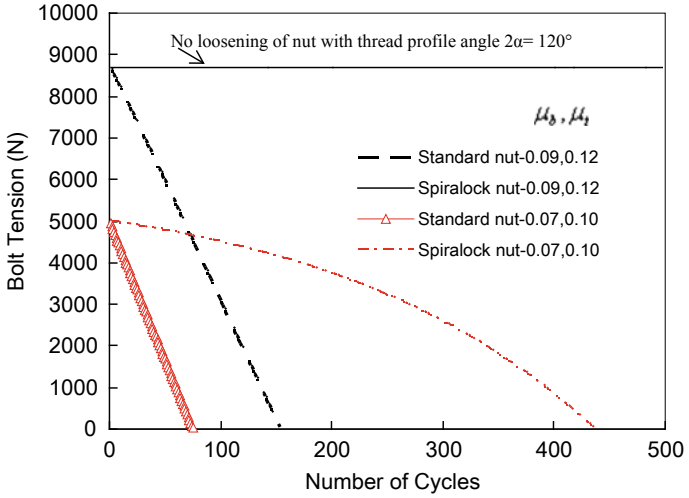

Fig. 9 Experimental validation of model prediction of nut loosening performance for two thread profile angles (standard nut with a thread profile angle $2\alpha = 60°$ versus nonstandard nut with $2\alpha = 120°$)

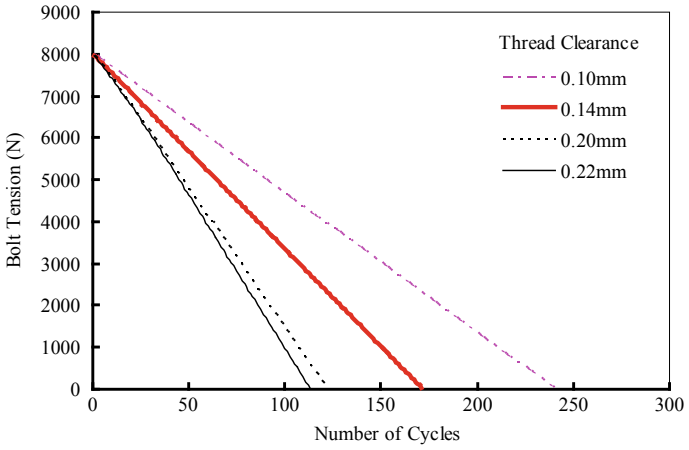

Fig. 10 Model prediction of the effect of thread clearance on the loosening performance of standard nut-bolt connection

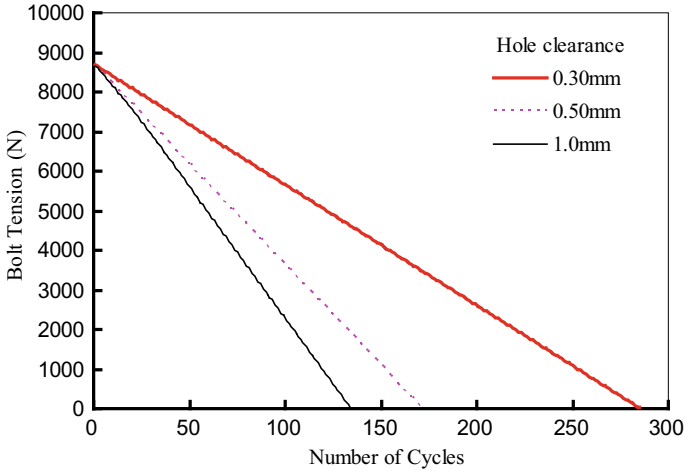

Fig. 11 Model prediction of the effect of hole diameter clearance on loosening performance of standard nuts

experimental values ranged from 0.065 to 0.13, for the various lubricity conditions between the underhead bearing and thread contact surfaces of test part. Bolt preload in this study is varied between 5 and 20.5 kN, which is 14–57% of the bolt proof load of 34.8 kN. Experimental validation of proposed model results on loosening performance was generated using a [modified] Junker vibration loosening test system [18] with a cyclic transverse displacement control.

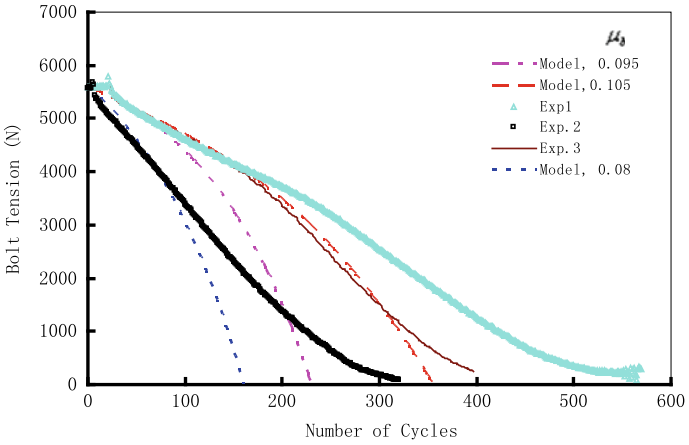

Fig. 12 Model validation of the loosening performance of nonstandard nut with thread profile angle $2\alpha = 120°$ (for bolt preload = 5600 N)

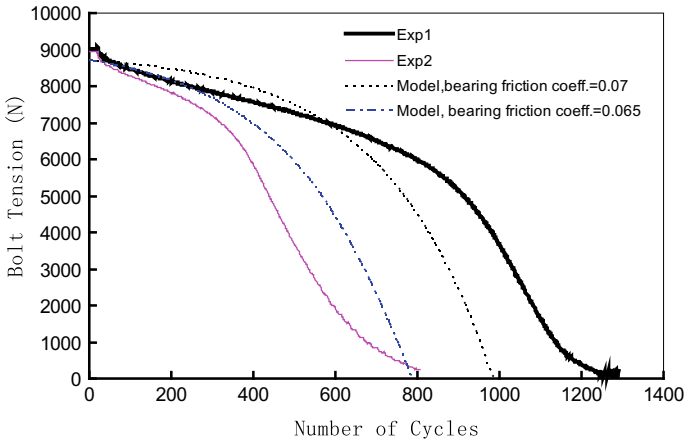

Fig. 13 Model validation of the loosening performance of nonstandard nut with thread profile angle $2\alpha = 120°$ (for bolt preload = 8,700 N)

3.1 Effect of Nut Thread Profile Angle 2α on the Loosening Performance

For the purpose of this study, two values of the nut thread profile angle $2\alpha = 120°$ and $2\alpha = 60°$ are used (Fig. 4) for engaging a standard bolt thread profile angle $2\alpha = 60°$. A commercially available specialty nut profile angle $2\alpha = 120°$ [7] is analytically and experimentally compared with standard female thread profile angle 600 [23] in terms of their respective loosening performance. For simplicity, it is

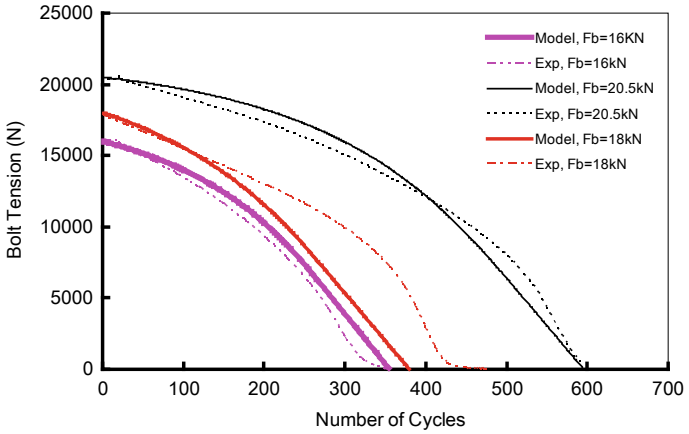

Fig. 14 Model validation of the effect of bolt preload on the loosening performance for standard nuts ($2\alpha = 60°$)

assumed that the thread friction coefficient μ_t would not be significantly affected by the thread profile angle, when test nuts have been cleaned.

Figure 8 displays the relationship between $\frac{T_t}{\mu_t F_b}$ and $\frac{F_{ts}}{\mu_t F_b}$ for the standard nut thread profile angle $2\alpha = 60°$ and nonstandard $2\alpha = 120°$ nuts when separately engaged with standard bolt threads. It is obvious that the ratio $\frac{F_{ts}}{\mu_t F_b}$ for critical transverse friction force of the larger thread profile angle nut ($2\alpha = 120°$) is much higher than that for the standard nut threads with $2\alpha = 60°$. If the transverse thread friction force F_{ts} is the same, the critical slipping thread friction torque T_t for $2\alpha = 120°$ would be much higher than that for standard nut. This means that the nut with larger thread profile angle is more resistant loosening as compared to nuts with standard thread profile angle $2\alpha = 60°$.

Figure 9 also shows better loosening performance of the nonstandard (larger) thread profile angle $2\alpha = 120°$, for various combinations of thread and bearing friction coefficients at two levels of bolt preload, namely 5000 and 8700 N. For an initial bolt preload of 8700 N the proposed model shows that the using a nut with a larger thread profile angle has completely prevented any loosening, while the standard nut $2\alpha = 60°$ has become completely loose (zero bolt tension) after only 150 vibration cycles. For a lower bolt preload of 5,000 N, the larger nut thread profile angle of $2\alpha = 120°$ has still out-performed the standard nut (with $2\alpha = 60°$) in terms of providing more resistance to loosening. The former withstood more than 400 vibration cycles before it became completely loose (with no residual bolt tension), as compared to less than 80 cycles for the latter.

3.2 Effect of Thread Fit

Figure 10 shows model prediction of the effect of thread fit clearance on the vibration loosening performance under harmonic transverse excitation. Thread fit class (tolerance) is often described as tight, medium, or loose fit [22]. An ISO designation of 6H/6g is assigned to a standard tolerance (fit) for commercially available metric nuts (6H)/bolts (6g). Since the nut thread clearance has already been directly incorporated as an independent variable in the proposed model, four arbitrary values of thread clearance are used, namely 0.10, 0.14, 0.20, and 0.22 mm. Results in Fig. 10 show that tighter thread fit would lower the rate of bolt loosing per cycle (i.e., increases the number of cycles to complete loosening). The number of the cycles until complete loosening is 240, 171, 121, and 113, for thread fit tolerance of 0.1 mm, 0.14 mm, 0.20 mm, and 0.22 mm, respectively.

3.3 Model Prediction of the Effect of Hole Clearance

Figure 11 shows loosening prediction of a of preloaded M10 $\times$ 1.5 bolt for hole diameter clearances of 0.3, 0.5, and 1.0 mm. A smaller hole clearance would reduce the vibration loosening rate, and the opposite is also true. For an initial bolt preload of 8700 N, the respective number of vibration cycles until complete loosening has been reached (i.e., zero bolt tension) for those three values of hole clearance are 285, 171, and 134.

3.4 Effect of Bearing Friction Coefficient on the Loosening Performance of Nuts with Nonstandard Thread Profile Angle ($2\alpha = 120°$)

Figures 12 and 13 show experimentally validated model prediction of the effect of bearing friction coefficient μ_b on the vibration loosening performance of a preloaded M10 $\times$ 1.5 bolt that is engaged with a nonstandard nut with a thread profile angle $2\alpha = 120°$ for two levels of bolt preload, namely 5600 and 8700 N. For both preload levels, the model prediction (solid lines) and experimental data (dotted lines) are in reasonable agreement in showing that increasing the bearing friction coefficient would reduce the bolt loosening rate per cycle. The difference between model prediction and the experimental data is lower for the higher preload level (Fig. 13).

3.5 Model Validation of the Effect of Bolt Preload

Finally, Fig. 14 shows experimental validation of the proposed model in terms of the effect of preload level on the loosening performance of a standard M10 × 1.5 bolt that is engaged with a standard nut ($2\alpha = 60°$). Three preload levels are used, namely 20, 18, and 16 kN; solid lines represent model prediction, while the dotted lines represent the corresponding experimental validation. Obviously, increasing the initial bolt tension would increase the number of vibration cycles-to-complete-loosening, in a nonlinear fashion. A reasonable agreement exists between the model prediction and test data.

4 Conclusion

This paper proposes an experimentally validated analytical model for investigating the effect of nut thread profile angle on the loosening performance of a preloaded bolt–nut system under a cyclic transverse excitation. Additional variables investigated include thread fit clearance, hole clearance, initial preload, and friction coefficients. Experimentally validated model prediction of the loosening performance shows that thread profile angle of the nut has significant effect on the loosening performance of a preloaded standard thread bolt. As compared to the standard nuts with 60° thread profile angle, nonstandard nuts with a larger thread profile angle of 120° (engaged with a preloaded standard M10 × 1.5 bolts) showed a significantly higher resistance to loosening under a harmonic transverse excitation. Results show also that reducing either of thread fit clearance (i.e., higher thread fit class) and/or reducing the clearance of bolt hole would increase the resistance to vibration-induced loosening of preloaded bolt–nut system. The opposite is also true; increasing either thread clearance (loose fit) and/or increasing the bolt hole clearance would reduce resistance to vibration-induced loosening of a preloaded bolt–nut system.

References

1. Ibrahim, R.A., Pettit, C.L.: Uncertainties and dynamic problems of bolted joints and other fasteners. J. Sound Vib. **279**, 857–936 (2005)
2. Harnchoowong, S.: Loosening of threaded fastenings by vibration, Ph.D. Dissertation. University of Wisconsin, Madison (1985)
3. Kasai, S., Matruoka, H.: Consideration of thread loosening by transverse impacts. ASME Press. Vessel. Pip. Div. PVP **367**, 117–123 (1998)
4. Kerley, J.J.: Dynamic and static testing of kaynar spiralock microdot nuts. Natl. Aeronaut. Space Adm. (NASA), Goddard Space Flight Cent. Eng. Serv. Div. Greenbelt MA (1984)
5. Junker, G.H.: New criteria for self-loosening of fasteners under vibration. SAE Trans. **78**, 314–335 (1969)
6. Finkelston, R.J.: How much shake can bolted joints take. Mach. Des. **44**, 122–125 (1972)

7. Hess, D.: Vibration and shock induced loosening. Handbook of bolts and bolted joints. In: Bickford, J.H., Nassar, S. (eds.) p. 911, pp. 757–824. Marcel Dekker, New York, NY (1998)
8. Sakai, T.: Investigations of bolt loosening mechanisms, 1st report: on bolts of transversely loaded joints. Bull. JSME **21**, 1385–1390 (1978)
9. Haviland, G.S.: Designing with threaded fasteners. Mech. Eng. **105**, 17–31 (1983)
10. Yamamoto, A., Kasei, S.: A solution for the self-loosening mechanism of threaded fasteners under transverse vibration. Bull. Jpn. Soc. Precis. Eng. **18**, 261–266 (1984)
11. Tanaka, M., Hongo, K., Asaba., E.: Finite element analysis of the threaded connections subjected to external loads. Bull. JSME **25**, 291–298 (1982)
12. Vinogradov, O., Huang, X.: On a high frequency mechanism of self-loosening of fasteners. In: Proceedings of 12th ASME Conference on Mechanical Vibration and Noise, Montreal, pp. 131–137. Quebec (1989)
13. Shoji, Y., Sawa, T.: Analytical research on mechanism of bolt loosening due to lateral loads. In: Proceedings of ASME Pressure Vessels and Piping Conference, Computer Technology, vol. 2, PVP2005–71333, pp. 59–65. Denver, Colorado, USA (2005)
14. Nassar, S.A., Housari, B.A.: Effect of thread pitch on the self-loosening of threaded fasteners due to cyclic transverse loads. ASME J. Press. Vessel. Technol. **128**, 590–598 (2006)
15. Nassar, S.A., Housari, B.A.: Study of the effect of hole clearance and thread fit on the self-loosening of threaded fasteners due to cyclic transverse loads. ASME J. Mech. Des. **128**, 586–594 (2006)
16. Housari, B.A., Nassar, S.A.: Effect of thread and bearing friction coefficients on the vibration-induced loosening of threaded fasteners under cyclic transverse loads. ASME J. Vib. Acoust. **129**, 1–9 (2007)
17. Nassar, S.A., Yang, X.: A mathematical model for vibration-induced loosening of preloaded threaded fasteners. ASME J. Vib. Acoust. **131**, 021009–1~13
18. Yang, X., Nassar, S.A.: Analytical and experimental investigation of self-loosening of preloaded cap screw fasteners. ASME J. Vib. Acoust. **133**, 031007–1~8
19. Motosh, N.: Development of design charts for bolts preloaded up to the plastic range. ASME J. Eng. Ind. **98**(3), 849–851 (1976)
20. Sopwith, D.G.: The distribution of load in screw threads. Proc. Inst. Mech. Eng. (G. B.) **159**(45), 373–383 (1948)
21. Englund, R.B., Johnson, D.H.: Finite element analysis of a threaded connection compared to experimental and theoretical research. J. Eng. Technol. **14**(2), 42–47 (1997)
22. Marks', L.S.: Standard handbook for mechanical engineers. In: Avallone, E.A., Baumeister, T. (eds.) III, 10th edn. pp. 8–21. McGraw-Hill, New York (1996)
23. Del, W.: From Earth to Saturn: getting a grip on vibration, shock and extreme temperature. Industrial and Utility Vehicle (January/February 2004)